Molecular Crystals and Liquid Crystals

ISSN: 1542-1406 (Print) 1563-5287 (Online) Journal homepage: http://www.tandfonline.com/loi/gmcl20

Modeling and simulation of physical sputtering

A. El Kebch, N. Dlimi, D. Saifaoui, A. Dezairi & M. El Mouden

To cite this article: A. El Kebch, N. Dlimi, D. Saifaoui, A. Dezairi & M. El Mouden (2016) Modeling and simulation of physical sputtering, Molecular Crystals and Liquid Crystals, 627:1, 183-189, DOI: 10.1080/15421406.2015.1137676

To link to this article: http://dx.doi.org/10.1080/15421406.2015.1137676

Published online: 13 May 2016.

MOL. CRYST. LIQ. CRYST.
2016, VOL. 627, 183–189
http://dx.doi.org/10.1080/15421406.2015.1137676

Taylor & Francis
Taylor & Francis Group

Modeling and simulation of physical sputtering

A. El Kebch[a], N. Dlimi[a], D. Saifaoui[a], A. Dezairi[b], and M. El Mouden[c]

[a]Laboratory of Theoretical and Applied Physics. Faculty of Sciences Ain Chock, Casablanca Morocco; [b]Faculty of Sciences Ben M'sik Casablanca Morocco; [c]Chouaib Doukkali University – Lab SIPE - National School of Applied Sciences (ENSA), El Jadida Morocco

ABSTRACT

In a thermonuclear fusion reactor Tokamak (ITER), the interaction of materials with the plasma to impact the creation of dust formed of beryllium (Be), tungsten (W) and carbon (C), result of erosion of the walls of the vacuum chamber by the plasma varying in size from a few nanometers to tens of microns and are highly reactive chemically.

In case of loss confinement, absorption of these microparticles could then result in consequences for the health of workers.

KEYWORDS

Modeling; plasma; erosion; sputtering

I. Introduction

Despite the plasma magnetic confinement, important flows of particles of the plasma towards walls are observed. Several effects are responsible for this transport.

⇒ Collisions between particles enable them to move from a magnetic field line to another. This is called neoclassical transport.

Some plasma instabilities are at the origin of a transport said abnormal. A particular type of instability is causing significant particle flux to the walls and proves very damaging as well:they are the ELM's (Edge Localized Mode) [1]. These instabilities occur when the tokomak operating in high confinement regime (H mode) [2]. This confinement regime, particularly successful, resulting in the existence of a zone Fort density gradient and temperature of the particles near the wall. An ELM corresponds to a quasi-periodic relaxation of the barrier which results in the release of a large amount of energy and particles in the direction of the wall.

Despite efforts to attempt to best manage these phenomena, they cannot be definitely avoided and must be taken into account in the design of future fusion reactors.

In operation of reactor, the walls are subjected to high energy particle flows.

Some are permanent, such as at the divertor or limiter. The materials the walls need to be very resistant to erosion and provide good heat dissipation deposited. For example, the limiter Tore Supra (France) is subject in the order of heat flux 15 MW/m^2 equivalent to the exhibition realized by the thermal shield of space shuttle entered the atmosphere.

CONTACT A. El Kebch alibec_ma@yahoo.fr Laboratory of Theoretical and Applied Physics, Faculty of Sciences Ain Chok, Casablanca, Morocco

Color versions of one or more of the figures in the article can be found online at www.tandfonline.com/gmcl.

These energy deposits are causing an erosion of the walls that engages different mechanisms:

⇒ Chemical erosion [3] is particularly important in hydrogen plasma and when the walls are made of carbon due to the high affinity hydrogen atoms. It becomes negligible for metal walls.

⇒ The physical sputtering [1] is due to the impact of ions on the wall. A part of their high kinetic energy when the impact is transferred to the material for the extraction of atoms from the surface.

These different process are the source of dust formation. These can be of various sizes and morphologies. It different from the spherical particles, agglomerates, flakes … …

The presence of dust in tokamaks has multiple negative effects [4]

⇒ The migration of dust in the heart of plasma can cause significant energy loss by bremsstrahlung (braking radiation).

This radiation is emitted when a charged particle is accelerated. It therefore place in permanently in tokamaks, even in the absence of dust. However, the intensity of the radiation emitted directly depends on the electric charges carried by the particles.

The presence of dust in tokamaks also problems the retention of fuel D-T. This phenomenon is particularly marked for dust composed of carbon, because of its high reactivity with hydrogen (and isotopes). Besides performance impairment, the retention is problematic in terms of tritium-related radioactivity ($t_{1/2} \simeq 12{,}3$ years). Redeposition of dust on the walls can lead to radioactive contamination of the chamber.

⇒ It exists also risk of explosion due to the presence of dust, [5] in case a discount to the brutal and accidental air of the chamber (flow of oxygen), or water leaks. These risks are especially important if the dust is composed of beryllium.

From this, it is obvious that both erosion and deposition of wall material will strongly determine the availability of ITER. It is therefore necessary to understand the involved mechanisms and to find possibilities to minimize erosion and deposition.

The erosion and deposition properties naturally depend on the material choice.

II. Erosion mechanisms

II.1. *The erosion yield Y*

To characterize the strength of erosion the yield Y is defined as ratio of the averaged number of eroded particles and number of incoming projectiles. It is important to mention that not a single projectile is considered but a large amount of projectiles such that the erosion yield represents the erosion probability. The yield can be determined by the flux of eroded particles Γ_{ero} divided by the flux of incoming projectiles Γ_{in} [6]

$$\Gamma_{in} = \frac{number\ \ of\ \ incoming\ \ projectiles}{are\ *\ time} \tag{2.1}$$

$$\Gamma_{ero} = \frac{number\ \ of\ \ eroded\ \ atoms}{are *\ \ time} \tag{2.2}$$

$$Y = \frac{\Gamma_{ero}}{\Gamma_{in}} \tag{2.3}$$

II.2. *Physical sputtering*

II.2.1. *Basic features [7.8]*

Within the process of physical sputtering, the momentum of incoming projectiles (energetic ions or neutrals) is transferred to surface atoms of the target material via nuclear collisions. If the transferred energy is large enough to overcome the surface binding energy (which is only known for a few materials, therefore it is common to use the heat of sublimation as an estimate), the surface atom can leave the solid and is physically sputtered. Although the first momentum transfer from projectile to target atoms is directed into the surface, subsequent collisions can lead to a momentum transfer which is directed out of the solid surface. Different regimes of collision can be distinguished mainly depending on the projectile energy and mass:

↪ *Single collision regime*
After one single collision of the projectile with a target atom the projectile hits a surface target atom. This process particularly occurs for light projectile ions with low energies.

↪ *Linear cascade regime*
Using mean projectile energies (larger than several10 eV) a collision cascade is developing in the solidincluding also the generation of recoil atoms. However, collisions between two moving atoms are rare.

↪ *Spike regime*

At high impact energies (keV – MeV) and high projectile masses the densities of recoils of the collision cascade is increasing. Inside the spike region most atoms are moving, whereby collisions between simultaneously moving particles become important.

Figure 1 illustrates these different regimes. The first two regimes can be described with the binary collision approximation.. However, under the conditions of wall materials in fusion experiments the spike regime is less important than the other two regimes.

Generally, physical sputtering occurs for all combinations of projectile and target materials.

The sputtered species are mostly neutral atoms or small clusters of the target material. Due to the nature of physical sputtering there exists a threshold energy for projectile ions below which the sputtering yield is zero. A surface atom at least has to receive the surface binding energy to be sputtered from the solid. Besides the impact energy the sputtering yield also depends on the impact angle of projectiles. Also the combination of projectile and substrate material influences the sputter yield.

II.2.2. *Physical sputtering yield*

In 1996, Y. Yamamura H. Tawara and [9] give a semi-empirical formula of sputtering based on the theory of Sigmund, valid for energies near the sputtering threshold If we consider an

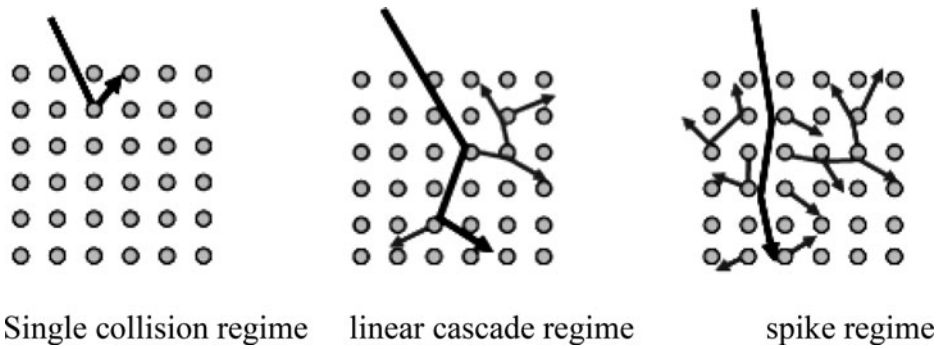

Figure 1. Collision regimes inside a solid induced by impact of a projectile atom.

incident particle of atomic mass M_1 and Z_1 atomic number, a target composed of atoms of atomic mass material M_2 and Z_2 atomic number, the sputtering rate for a normal incidence Y (E) is written:

$$Y(E) = 0.042 \frac{Q(Z_2).\alpha^*(M_1/M_2)}{U_s} \times \frac{S_n(\varepsilon)}{1 + \Gamma k_e \varepsilon^{0.3}} \times \left[1 - \sqrt{\frac{E_{th}}{E}}\right]^2 \tag{2.4}$$

E is the energy in (eV) and where ε the Reduced energy:

$$\varepsilon = \frac{0.03255}{Z_1 Z_2 (Z_1^{2/3} + Z_2^{2/3})^{1/2}} \times \frac{M_2}{M_1 + M_2} E \tag{2.5}$$

$S_n(\varepsilon)$ and $k_e \varepsilon^{0.3}$ are respectively the nuclear and electronic stopping powers.

U_s is the energy of sublimation which is assumed equal to the binding energy.

The factor used to weight the electronic stopping power depending on the mass of the incident particle.

Indeed, the energy loss by collisions with electrons of the material is not negligible for light ions. This factor is:

$$\Gamma = \frac{W(Z_2)}{1 + (M_1/7)^3} \tag{2.6}$$

such as :

$$S_n(\varepsilon) = \frac{84.78 Z_1 Z_2}{(Z_1^{2/3} + Z_2^{2/3})^{1/2}} \times \frac{M_1}{M_1 + M_2} s_n(\varepsilon) \tag{2.7}$$

and

$$k_e = 0.079 \frac{(M_1 + M_2)^{3/2}}{M_1^{3/2} \times M_2^{1/2}} \times \frac{Z_1^{2/3} \times Z_2^{1/2}}{(Z_1^{2/3} + Z_2^{1/2})^{3/4}} \tag{2.8}$$

Where W is an empirical parameter, characteristic of the material.

α^* depending on the mass ratio M_1/M_2 and is inelastic collisional phenomena.

He was tabbed for many couples projectile/target which allows to obtain a smoothed Yamamura formula for this coefficient:

$$\alpha^* = 0.249 \times \left(\frac{M_2}{M_1}\right)^{0.56} + 0.0035 \times \left(\frac{M_2}{M_1}\right)^{1.5} \text{ pour } M_1 \geq M_2 \tag{2.9}$$

$$\alpha^* = 0.0875 \times \left(\frac{M_2}{M_1}\right)^{-0.15} + 0.165 \times \left(\frac{M_2}{M_1}\right) \text{ pour } M_1 \leq M_2 \tag{2.10}$$

The sputtering threshold Eth was also tabulated from experimental data.

Yamamura in then gives a general expression in which this coefficient depends only on the binding energy and mass of the projectile and target:

$$\frac{E_{th}}{U_s} = \frac{6.7}{\gamma} \qquad \text{Pour } M_1 \geq M_2 \tag{2.11}$$

$$\frac{E_{th}}{U_s} = \frac{1 + 5.7 \times (M_1/M_2)}{\gamma} \qquad \text{Pour } M_1 \leq M_2 \tag{2.12}$$

withe

$$\gamma = \frac{4 M_1 M_2}{(M_1 + M_2)^2} \tag{2.13}$$

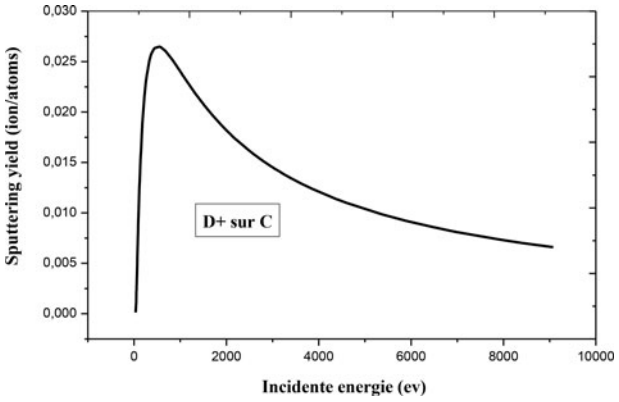

Figure 2. Calculated sputtering yield for D^+ on C : energy dependence.

$$E_{th}(\theta) = U_s \left[4.4 - 1.3 \log(m_2/m_1\right] \cos^2(\theta) \tag{2.14}$$

U_s is the energy of sublimation (eV), m_1 and m_2 respectively the masses of the incident particle and the target particle.

III. Results and discussion

III.1. *Physical sputtering rate*

Figures 2,3,4 show the effect of the energy of the impact on the physical sputtering yield of beryllium, carbon and tungsten because of deuterium at normal incidence calculated using the Monte Carlo technique.

For impact energies above the threshold energy physical sputtering occurs with the sputter yield increasing monotonically until reaching a maximum value at a certain impact energy: more energy can be transferred to surface atoms, which increases the probability for sputtering. Further increase of the impact energy leads to continuous decrease of the sputter yield: the impinging projectiles and therefore also the collision cascades penetrate deeper into the solid and therefore less energy is transferred to surface atoms.

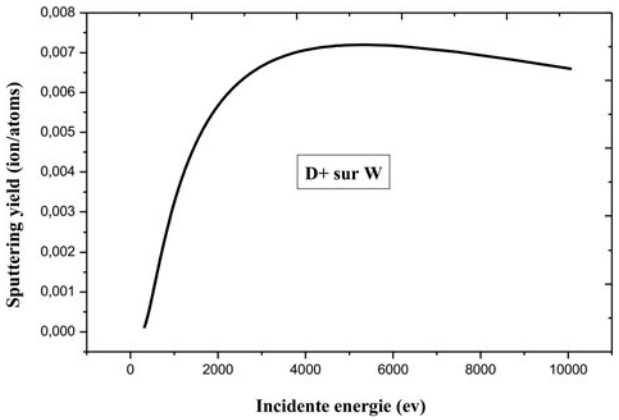

Figure 3. Calculated sputtering yield for D^+ on W energy dependence.

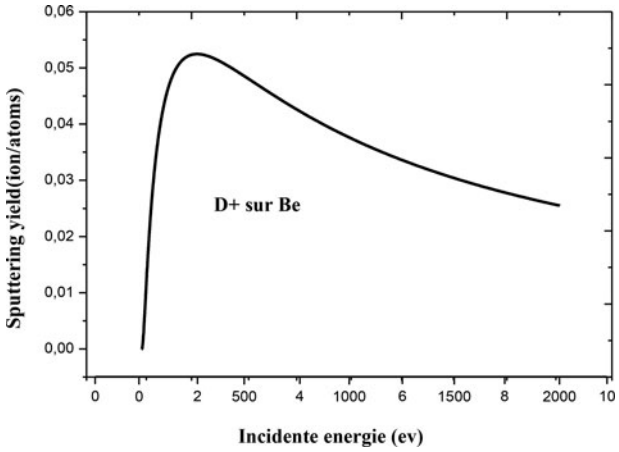

Figure 4. Calculated sputtering yield for D^+ on Be energy dependence.

III.2. *Angular dependence of Y_{phys} for different threshold energy*

Figure 5 shows the effect of the angle of incidence on the physical sputtering yield for different threshold energy.

The angle of incidence α of projectiles from hitting the surface is defined as the angle between the velocity vector of the projectile and the normal vector to the surface.

Figure 5 shows the physical sputtering yield calculated for deuterium on tungsten for fixed impact energy (first case E = 250 eV, 2nd case E = 350 eV and 3rd case E = 500 eV) in dependence on the angle of incidence.

From normal incidence the sputter yield increases with increasing angle of incidence.. After reaching a maximum yield.

Table 1 shows the incidence angle corresponds to the maximum physical sputtering yield.

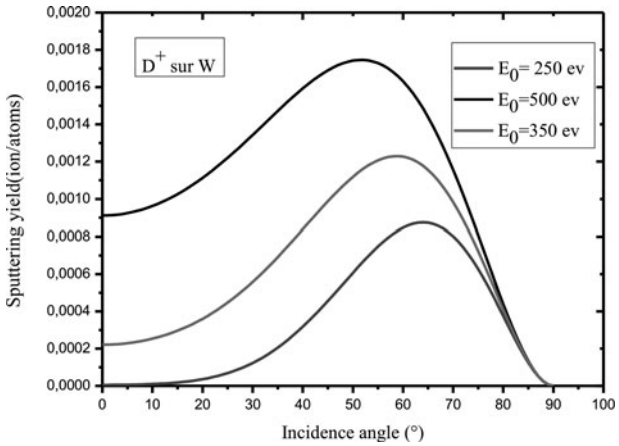

Figure 5. Calculated sputtering yield for D on W: angular dependence.

Table 1. The incidence angle corresponds to the maximum physical sputtering yield.

Incidence energie	250 eV	350 eV	500 eV
Physical sputtering yield	$8.75.10^{-4}$	0.00123	0.00175
Incidence angle	64°	59°	52°

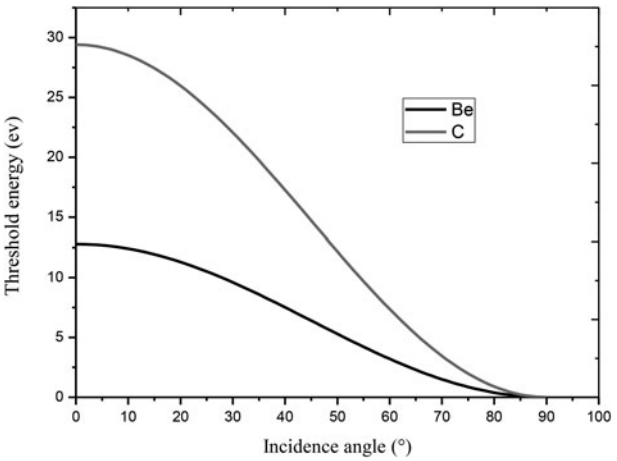

Figure 6. Variation the sputtering threshold as a function of the angle of the incident.

III.3. *Angular dependence of threshold energy*

In Figure 6, the sputtering threshold varies a function of the angle of incident particles to the walls. For small angles, the sputtering threshold and higher than for the biggest angles of incidence.

This means that the particles arriving on the walls with of small incidence angles must have a very high energy to be able to pulverizing the surface of the walls.

VI. Conclusion

The most important sputtering and erosion mechanisms occurring in fusion experiments have been described. Physical sputtering takes place for all combinations of projectile and target but disappears at low impact energies below a threshold (around several eV). Under most conditions physical sputtering can be described by collision cascades inside the solid initiated by the impinging projectile. Using the binary collision approximation. However, at low impact energies ($< \sim$10eV). The sputtering yield for high-atomic number materials is in general smaller than for low- atomic number materials.

References

[1] Zohm, H. (1996). *Plasma Phys. Control. Fusion*, *38*, 105–128.
[2] Wagner, F., Becker, G., Behringer, K., Campbell, D., Eberhagen, A., Engelhardt, W., Fussmann, G., Gehre, O., Gernhardt, J., Gierke, G. v., Haas, G., Huang, M., Karger, F., Keilhacker, M., Kluber, O., Kornherr, M., Lackner, K., Lisitano, G., Lister, G. G., M.Mayer, H., Meisel, D., Muller, E. R., Murmann, H., Niedermeyer, H., Poschenrieder, W., Rapp, H., Rohr, H., Schneider, F., Siller, G., Speth, E., Stabler, A., Steuer, K. H., Venus, G., Vollmer, O., & Yu, Z. (1982). *Phys. Rev. Lett.*, *49*, 1408–1412.
[3] Kleyn, A.W., Koppers, W., & Lopes Cardozoa, N. (2006). *Vacuum*, *80*(10) :1098–1106.
[4] Federici, G., Skinner, C. H., Brooks, J. N., Coad, J. P., Grisolia, C., Haasz, A. A., Hassanein, A., Philipps, V., Pitcher, C. S., Roth, J., Wampler, W. R., & Whyte, D. G. (2001). *Nucl. Fusion*, *41* :1967–2137.
[5] Sharpe, J. P., Petti, D. A., & Bartels, H. W. (2002). *Fusion Engineering and Design*, *63–64*, 153–163.
[6] Kirschner, A. (2008). *Transactions of Fusion Science and Technology*, 53.
[7] Eckstein, W. (1991). *Computer simulation of ion-solid interactions*. Springer-Verlag: Berlin, Heidelberg and New York.
[8] Chapman, B. (1980). *Glow discharge processes*. John Wiley & Sons: New York.
[9] Yamamura, Y., & Tawara, K. (1996). *Atomic-Data-and-Nuclear-Data-Tables*, 62 (2), 149.